# Gyrokinetic investigation of isotope effect on flow oscillations in ohmic tokamak discharges

P. Niskala [1], T.P. Kiviniemi[1], S. Leerink[1], T. Korpilo[1]

[1]*Department of Applied Physics, Aalto University, Espoo, Finland*

## 1. Introduction

Improved confinement has been measured in deuterium plasmas compared to hydrogen discharges with similar parameters [1]. This ”isotope effect” runs counter to the general understanding of heat and particle transport in plasmas. Turbulence is held as the main culrpit for anomalous transport observed in tokamaks, and one would expect the increased ion mass to boost transport and thus lead to deterioration of confinement.

On the other hand, many theories on L-H transition rely on radial flow shear to suppress the turbulent transport [2]. A variety of mechanisms affect the flows in plasmas, creating mean and zonal flows. The latter ones include the geodesic acoustic mode (GAM), a time-varying radial oscillation of potential. Given the connection between flows and the plasma confinement, possible effects of ion species on the GAM dynamics have gathered interest. We study the isotope effect on GAMs via gyrokinetic full-f simulations of hydrogen and deuterium discharges from the FT-2 tokamak. Here we present the analysis of two particular discharges from the computational point of view, while combining simulations with experimental observations is discussed by Gurchenko et al [3].

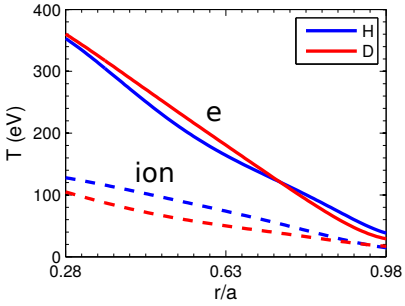


Figure 1: *Deuterium case had a higher $T_e/T_i$ ratio. The $O^{6+}$ impurities have same temperature as the main ions.*

## 2. Simulation setup

The simulations were conducted using ELMFIRE, a gyrokinetic code simulating coupled neoclassical and turbulent dynamics [5, 6, 7]. ELMFIRE uses the particle-in-cell method to model the evolution of full plasma distribution function plasma. The distribution is initialised as particles on a toroidal grid according to initial input profiles for density and temperature. A total of three particle species can be included in the calculations: electrons and two ions. Collisions between the particles have been implemented using a binary collision model.

At every time step, charge densities are distributed to the grid. Particle movement utilizes as a hybrid explicit-implicit pusher. The explicit step produces charge separation, which is then used

Table 1: *Simulation parameters.*

| Isotope | $B_\phi$ (T) | $I_0$ (kA) | $T_e$ (eV) | $T_i$ (eV) | $n_e$ ($10^{19}$ m$^{-3}$) | $Z_{\text{eff}}$ |
|---|---|---|---|---|---|---|
| H | 2.27 | 20.5 | 416 | 147 | 2.68 | 2.3 |
| D | 2.22 | 19.4 | 435 | 151 | 2.48 | 2.8 |

to solve the electric potential to ensure quasineutrality. The potential is interpolated to particles to calculate the polarisation drift on ions and parallel electric field acceleration on both ions and electrons in the implicit step.

The magnetic geometry of ELMFIRE is fixed as co-centric flux surfaces with no shifts. Simulation region is limited radially, resulting in a toroidal annulus. Electric field is set to zero at the inner boundary and potential to zero at the wall. Toroidal magnetic field on the magnetic axis and the current profile are given as an input to determine the total magnetic field and safety factor profile.

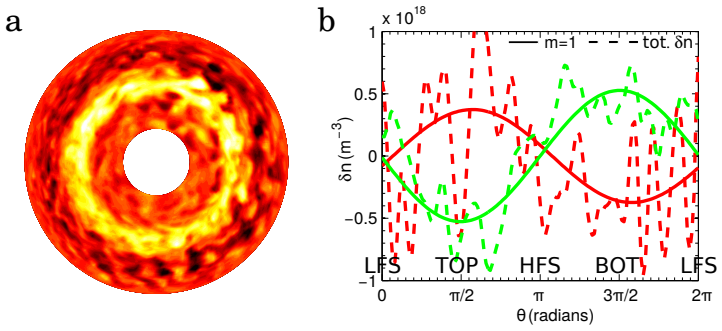


Figure 2: *The poloidal snapshot of (a) shows the characteristic temporally varying GAM oscillation, while the $m = 1$ density fluctuation is visible for opposite temporal phases in (b).*

The simulations are based on two plasma discharges from the FT-2 tokamak ($a = 0.08$ m, $R_0 = 0.55$ m), denoted here on as just hydrogen (H) and deuterium (D). The basic parameters are presented in table 1. Besides the isotope, main difference between the cases comes from the effective charge number $Z_{\text{eff}}$ and ion temperature, as seen in figure 1. Partially ionised oxygen ($O^{6+}$) was taken included as the impurity ions in the simulations, and the density profile was initialised according to the effective charge. Simulation grid spanned radially from $r = 0.02$ m to $r = 0.08$ m with 120 radial, 150 poloidal and 8 toroidal grid points. A total of approximately $10^9$ particles was initialised with a simulation time step of 0.03 microseconds.

### 3. Simulation results

The main features of geodesic acoustic mode are clearly visible in the simulations. Firstly, the expected radial oscillation is evident in the results for the electric potential, as seen in figure 2a. The temporal frequency for these dominating fluctuations is smaller for deuterium (below 50 kHz), as would be expected based on simplest analytical expressions for frequencies [4]. The frequency is largely constant in radial direction. Secondly, fluctuations are also present in the radial electric field, which couples the potential oscillation to a sinusoidal $m = 1$ mode in density. Figure 2b shows that this mode is clearly present in the simulations as density fluctuations at the characteristic GAM frequency.

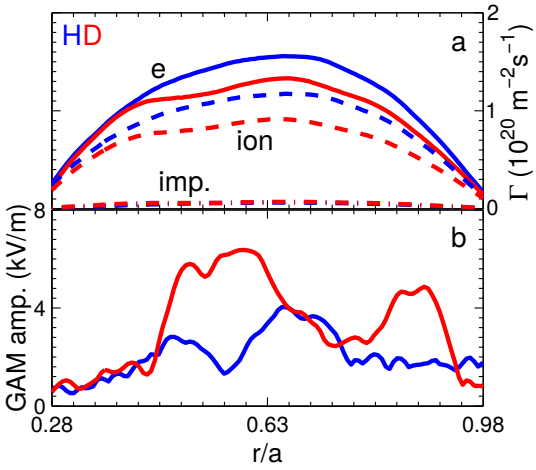


Figure 3: *Particle fluxes are larger for hydrogen (a), while $E_r$ oscillations at the GAM frequency have a higher amplitude for the deuterium case (b).*

The amplitude of the temporal $E_r$ oscillations is distinctly higher for deuterium, as figure 3b demonstrates. Similar trend has been observed for zonal flows at TEXTOR [8]. The amplitudes have large spatial variation, with the strongest oscillations located close to the middle plasma radius. The amplitude of the $m = 1$ density oscillations scales similarly, indicating that the top-bottom asymmetry is captured in the simulations. The radial wavelength of the oscillations also increases from deuterium to hydrogen, consistently with both earlier simulations and theoretical work [9, 10]. Based on the theoretical work by Hahm et al [11], higher amplitude combined with lower frequency could lead to higher effective shearing rate and stronger reduction of turbulence for deuterium.

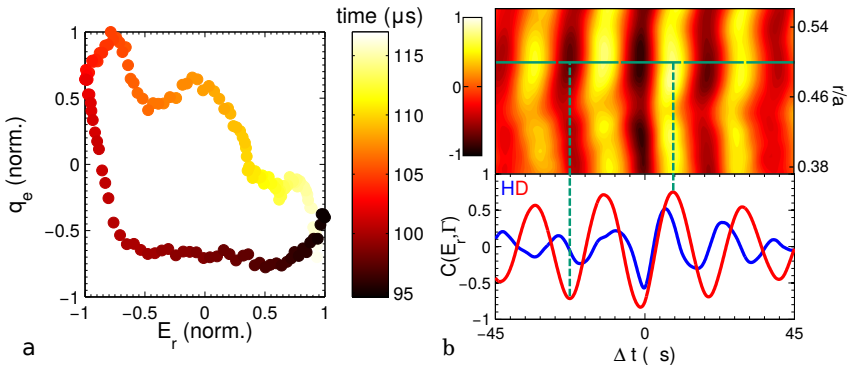


Figure 4: *Flux and $E_r$ oscillations have limit-cycle-like characteristics, especially for the deuterium case (a). Correlation between $E_r$ and particle flux is stronger and less localised for deuterium compared to hydrogen (b).*

Hydrogen simulation produces larger energy fluxes, but conductive heat fluxes are similar for both isotopes. The difference is explained by particle fluxes, which are seen as the temporal mean levels in figure 3a. Generally it is difficult to attribute decreased particle fluxes to the stronger $E_r$ oscillations of the deuterium case, but there is a slight dip in the region where $E_r$ has the highest amplitude. Furthermore, $E_r$ and transport oscillations have a predator-prey-like phase shift in the simulations, as seen in the single oscillation period of figure 4a . Figure 4b demonstrates that this correlation between the two is also more distinct for deuterium. Moreover, the correlation is less localised for deuterium. These observations are compatible with increasing GAM amplitude and radial wavelength, but temporal standard deviation of flux oscillations grows slightly as well, indicative of the relationship between transport and $E_r$.

## 4. Discussion

While the simulations show the deuterium plasma to have stronger geodesic acoustic mode activity and increased correlation with transport, there is room for more detailed investigations. The computational study can be expanded by including more cases to further establish the trends in transport and amplitudes. Additionally, GAM wavelength and propagation at FT-2 deviates from the theoretical predictions of Itoh et al. Investigating the characteristics and scaling of the GAMs observed in FT-2 via ELMFIRE simulations offers an appealing avenue for deepening the understanding of flow dynamics in tokamak plasmas, bridging the theoretical and experimental observations through advanced computations.

**Acknowledgements:** We thank A.D. Gurchenko for E.Z. Gusakov for providing experimental input data. This work was supported by grant 278487 of the Academy of Finland has received funding from Tekes – the Finnish Funding Agency for Innovation. Computational resources for the work were provided by CSC - IT Center for Science and IFERC.

## References

[1] M. Bessenrodt-Weberpals et al, Nuclear Fusion **33**, 1205 (1993)

[2] P.W. Terry et al, Reviews of Modern Physics **72**, 109 (2000)

[3] A.D. Gurchenko et al, I5.J203 at this conference

[4] N. Winsor et al, Physics of Fluids **11**, 2448 (1968)

[5] J.A. Heikkinen et al, Journal of Computational Physics **227** (2008)

[6] S. Leerink et al, Physical Review Letters **109**, 165001 (2012)

[7] T.P. Kiviniemi et al, Plasma Physics and Controlled Fusion **56**, 075009 (2014)

[8] Y. Xu, Physical Review Letters **110**, 265005 (2013)

[9] P. Niskala et al, Nuclear Fusion **55**, 073012 (2015)

[10] K. Itoh et al, Plasma and Fusion Research **1**, 037 (2006)

[11] T.S. Hahm et al, Physics of Plasmas **6**, 922 (1999)